Cangnan County, Wenzhou City, China are determined by conducting triaxial and consolidation tests based on different moisture contents. The main conclusions of the study are obtained.

(1) Different water-bearing states caused by shallow gas in reservoirs significantly affect the shear strength of the muddy clay with thin silt interlayers. *c* of the soil presents a ladder-type steep reduction as soil moisture content increases, but φ has a weaker correlation with the moisture content.

(2) The overall strength characteristics of the muddy clay with thin silt interlayers are determined by the combined action of the muddy clay and the thin silt interlayers. The soil with different moisture contents presents relatively linear elastic properties at a small strain. The stress-strain curve of the soil alternates between mild strain hardening and mild strain softening as soil moisture content varies.

(3) As moisture content decreases, E_s of the muddy clay with thin silt interlayers gradually increases, but the coefficient of compressibility decreases. The average moisture content and the thin silt interlayers slightly influence the overall deformation characteristics of the soil.

ACKNOWLEDGMENTS

This work was financially by the National Natural Science Foundation of China (51109208), the Foundation of State Key Laboratory for Geomechanics and Deep Underground Engineering (SKLGDUEK1110), the Natural Science Foundation of Hubei Province, China (2011CDB407).

REFERENCES

Adams, N. and Kuhlman, L.G. (1991). "How to prevent or minimize shallow gas blowouts." *World Oil*, 212(5): 51-60.

Bernard, P.B., Chris, A. and Bruce, D.J. (2005). "Bubble growth and rise in soft sediments". *Geological Society of Americ*a, 33(6): 517-520.

Ding, G.S., and Tian, X.Y. (1996). "China's shallow gas resources and exploration prospects".*Oil & Gas Geology*, 17(3): 226-231.

Eigenbrod, K.D and Burak, J.B. (1991). "Effective stress paths and pore-pressure responses during undrained shear along the bedding planes of varved Fort William Clay.". *Canadian Geotechnical Journal*, 28(6): 804-811.

Feng, M.Z., Ji, J. (2006). "The geological hazard evaluation by shallow layered natural gas in Shanghai region". *Shanghai Geology*, 100(4): 44-47.

Garcia, G.A., Orange, D.L., and Miserocchic, S., et al. (2007). "What controls the distribution of shallow gas in the Western Adriatic Sea? " *Continental Shelf Reaearch*, 27(3-4): 359-374.

George, H. (1986)."Characteristics of varved clays of the Elk Valley, British Columbia, Canada." *Engineering Geology*, 23(1): 59-74.

Guo, A.G., Kong, L.W., and Shen, L.C., et al. (2013). "Study of disaster countermeasures of shallow gas in metro construction. " *Rock and Soil Mechanics*, 34(3): 769-775.

Huang, J.M, Gu, Y., and Mao, H.M. (2008). "Study on construction technology for jacking of concrete pipe through shallow gas stratum". *Building Construction*,

30(3): 222-225.
Hughen, K.A., and Zolitschka, B. (2007). "Varved marine sediments.". *Encyclopedia of Quaternary Science*, Elsevier Science Ltd, Kidlington: 3114-3132.
Jiang, Y., Tian, M.Y. (2003). "Prediction of subsidence caused by exploiting oil and gas. " *Journal of Liaoning Technical University*, 22(6): 746-748.
Kong, L.W., Guo, A.G., Chen, S.Y., and et al. (2004). "Influence of shallow natural gas blow out on stratum damage and hazard analysis of pile foundation". *Journal of Disaster Prevention and Mitigation Engineering*, 24(4): 375-381.
Lin, C.M., Li, Y.L., Zhuo, H.C., and Zhang, Z.P., et al. (2009). "Geology and pore-water pressure sealing of shallow biogenic gas in the Qiantang River incised valley fills". *Journal of Palaeogeography*, 11(3): 314-329.
Sills, G.C., and Gonzalez, R. (2001). "Consolidation of naturally gassy soft soil". *Geotechnique*, 51(7): 629-639.
Stermac, A.G., Lo, K.Y., and Barsvary, A.K.(1967). "The performance of an embankment on a deep deposit of varved clay". *Canadian Geotechnical Journal*, 4(1): 45-61.
Wheeler, S.J. (1988). "A conceptual model for soils containing large gas bubbles". *Geotechnique*, 38(3): 389-397.
Wang, Y., Kong, L.W., Guo, A.G., et al. (2010). "Effects of gas release rate on gas-water migration in shallow gas reservoir". *Journal of Zhejiang University (Engineering Science)*, 44(10): 1883-1889.
Xie, C.Y. (2005). "Shallow gas along the Yangtze river in Anhui province and its effects on hydraulic structures". *Express of Water Resources & Hydropower Information*, 21(10): 11-16.
Ye, N.J., Li, G.J. (2008). " Research on influence of shallow-buried natural gas on pile foundation of bridge and its countermeasures". *Highway*, (12): 61-64.
Zimmerman, D. (2009). "Investigation report of oil and gas leasing in the outer continental shelf". Northcoast Ocean and River Protection Association.
Zolitschka, B. (2007). "Varved lake sediments.". *Encyclopedia of Quaternary Science*, Elsevier Science Ltd, Kidlington: 3105-3114.

Analysis of Surrounding Rock Displacement Induced by Tunnel Excavation in Horizontal Interbedding Rock Mass

Yong Fang[1], Ya-peng Fu[2], Bin Yang[2], Ge Cui[2] , Xiao-min Wang[2]

[1]Associate Professor, Key Laboratory of Transportation Tunnel Engineering, Ministry of Education, Dept. of Civil Engineering, Southwest Jiaotong University, Chengdu 610031, China, Email: fy980220 @swjtu.cn
[2]Master candidate, Key Laboratory of Transportation Tunnel Engineering, Ministry of Education, Dept. of Civil Engineering, Southwest Jiaotong University, Chengdu 610031, China, Email: fyp19900328@foxmail.com, 285525675 @qq.com, cuige114 @126.com, 410504236@qq.com

ABSTRACT: Material properties of horizontal sandstone and mudstone interbedding rock mass have significant differences in the horizontal and vertical directions. It is difficult to reveal the characteristic of surrounding rock displacement induced by tunnel excavation in horizontal interbedding rock mass by numerical methods based on isotropic constitutive models. Regarded as transversely isotropic medium, material parameters such as density, elastic modulus, poisson ratio etc. of interbedding rock mass are deduced. As an example, transversely isotropic constitutive model is taken into consideration in three dimensional numerical model of Luan Jiayan tunnel on Guangnan highway. The process of tunnel excavation is simulated in this model, and ground displacement distribution and variation with excavation steps are obtained. For the purpose of comparison, field tests of vault settlement and side wall convergence caused by tunnel construction are carried out. It is shown that compared with isotropic constitutive model, transversely isotropic constitutive model can reflect the physical difference in horizontal and vertical directions for interbedding rock mass of sandstone and mudstone. But transversely isotropic model is elastic, and plastic zone caused by tunnel excavation can't be obtained. So there exist some differences from actual situation when this model is applied.

INTRODUCTION

In general, we regard sedimentary rock whose stratum bedding-plane is approximately level as horizontal stratum, and the altitude of the same rock formation for horizontal stratum is basically the same. In the process of Guangyuan-Nanchong expressway construction, tunnels are built to pass through mountainous region in the Sichuan Basin. Stratigraphic dip angle in tunnel site area is low and nearly horizontal;

rock strata is sandstone and mudstone interbedding rock mass, the differences of rock properties are significant, and the rock stratum possesses typical transverse isotropic characteristics. During the excavation of tunnel, the deformation mechanism of surrounding rock and the mechanical behavior characteristics of lining structure are rather different from common rock.

Xian Mowen (1995) verified the stability and feasibility of excavation scheme of four parallel canal tunnel through Limestone and shale interbedding rock mass. B.L.Chu (2007) took the conditions of homogeneous surrounding rock, 2-layer surrounding rock and 3-layer surrounding rock into consideration, conducted the model and numerical experiments of two circular tunnel excavation, analyzed the mechanical behavior of the cavern after excavation. Based on the construction monitoring results, Guan Huiping (2008) analyzed the reasons and characteristics of the surrounding rock deformation for horizontal rock tunnel surrounding rock deformation, and discussed the classifications of the deformation stages. YanLi (2009) regarded each rock stratum as the isotropic continuous medium, considered the influence of rock stratum interface, performed the numerical model and discussed the stability of middle rock pillar. In addition, the influences of the different net distances between two tunnels and the various surrounding rock conditions on the stability of middle rock pillar are studied. Based on Biot's theory of consolidation, the time-dependent analytical solutions of stress, displacement and pore pressure induced by circular tunnel excavation in a transversely isotropic and saturated soil were obtained by LiuGanbin (2003) in the Laplace transform domain. The anisotropic elastoplastic model of layered soil was established by ZhuYanzhi (2005) to solve seismic response analysis of shield tunnel systems in layered soil. Transversely isotropic characteristics of the segment structure were taken into consideration, and impacts on the existing tunnel caused by the construction of parallel and undercrossing shield tunnels was simulated by FangYong (2007).

Due to the numerous structure planes of horizontal sandstone and mudstone interbedding rock mass (2006,2010) and the typical transversely isotropic characteristics, it is difficult to reveal the characteristic of surrounding rock displacement induced by tunnel excavation in horizontal interbedding rock mass by numerical methods based on isotropic constitutive models. In this paper, by introducing transversely isotropic theory, surrounding rock displacement induced by excavation is studied when the tunnel passes through horizontal sandstone and mudstone interbedding strata.

TRANSVERSELY ISOTROPIC CONSTITUTIVE MODEL

Basic Assumptions

For horizontal soft-hard interbedding rock layer, each individual layer possesses approximately isotropic characteristics, but from the overall point of view, elastic modulus are greatly different in the horizontal and vertical directions, which means that interbedding stratum owns transversely isotropic characteristics. To deduce the constitutive model of horizontal soft-hard interbedding rock mass, the following assumptions are necessary.

①The rock layers bond firmly and don't produce sliding displacements, which is in accordance with the consistent deformation theory ;

②each individual layer is isotropic medium.

The equivalent model of nearly horizontal strata includes three equivalent physical parameters, namely density, elastic modulus and poisson ratio.

Surrounding Rock Density

According to the fact that the total weight and volume of equivalent surrounding rock are equal to the original interbedding surrounding rock, there is such formula as follows:

$$\sum_{i=1}^{n} \rho_i g h_i = \rho g h \tag{1}$$

The equivalent stratum density is:

$$\rho = \sum_{i=1}^{n} \rho_i h_i \Big/ \left(\sum_{i=1}^{n} h_i \right) = \sum_{i=1}^{n} \rho_i h_i \Big/ h \tag{2}$$

Where, ρ_i and h_i are the density and thickness of each stratum, h is the thickness of equivalent stratum,n is the number of strata, and ρ is equivalent density.

Elastic Modulus

(1) E_v: equivalent elastic modulus in the vertical direction.

Figure 1 shows the derivation for equivalent elastic modulus in the vertical direction. Where, E_i is the elastic modulus of surrounding rock, and E_v is the equivalent elastic modulus.

By the action of a vertical unit load F on interbedding strata and equivalent stratum, according to the fact that vertical compression displacements of two models produced by the unit load are equal, there is such formula as follows:

$$\sum_{i=1}^{n} \left[F/(E_i L/h_i) \right] = F/(E_v L/h) \tag{3}$$

The calculation formula for vertical elastic modulus is

$$E_v = h \Big/ \left(\sum_{i=1}^{n} h_i / E_i \right) \tag{4}$$

(2) E_h: equivalent elastic modulus in the horizontal direction.

Figure 2 shows the derivation for equivalent elastic modulus in the horizontal direction. Where, E_i is the elastic modulus of surrounding rock, and E_h is the equivalent elastic modulus.

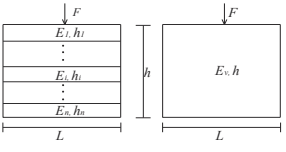

Fig. 1 Vertical elastic modulus

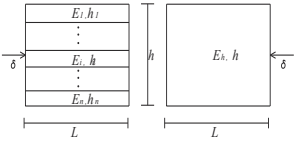

Fig. 2 Horizontal elastic modulus

By the action of a horizontal unit displacement δ on originally interbedding strata and equivalent stratum, this displacement would result in horizontal pressure, and according to the fact that the horizontal pressure of two models produced by the unit displacement are equal, there is such formula as follows:

$$E_h h\delta / L = \sum_{i=1}^{n} E_i h_i \delta / L \tag{5}$$

The calculation formula for horizontal elastic modulus is

$$E_h = (\sum_{i=1}^{n} E_i \mathrm{h}_i) \Big/ h \tag{6}$$

Poisson Ratio

In the transversely isotropic medium, the poisson ratio includes two parameters: and, which respectively represent the poisson ratio in the vertical and horizontal directions. Poisson ratio of equivalent model can be calculated according to the horizontal pressure and vertical pressure ratio. In the transversely isotropic elastic medium, lateral pressure coefficient is defined as:

$$\lambda' = \sigma_x / \sigma_y = E_h \nu_{vh} / [E_v (1 - \nu_{hh})] \tag{7}$$

Figure 3 shows the equivalent model of poisson ratio. Both of the original soil and equivalent soil are under vertical pressure F, two sides are restricted by the horizontal constraints, and bottom is restricted by vertical constraints.

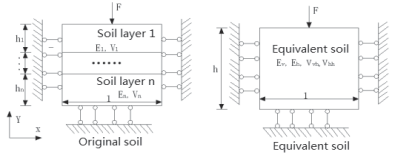

Fig. 3 Equivalent model 1 of poisson ratio

In the boundary conditions, the horizontal total pressure of interbedding strata is: $\sum_{i=1}^{n} (\lambda_i F h_i) / L$, the horizontal total pressure of equivalent stratum is: $(\lambda' F h) / L$. In theory, they are equal to each other.

$$\sum_{i=1}^{n} (\lambda_i F h_i) / L = (\lambda' F h) / L \tag{8}$$

Where is the lateral pressure coefficient, the further result is as follow:

$$\nu_{vh} \Big/ (1 - \nu_{hh}) = h \sum_{i=1}^{n} [\nu_i h_i / (1 - \nu_i)] \Big/ [(\sum_{i=1}^{n} E_i h_i)(\sum_{i=1}^{n} \frac{h_i}{E_i})] \tag{9}$$

Similarly, horizontal compression displacements of the equivalent stratum model and all original strata are δ, as is shown in figure 4, the left side is restricted by the horizontal constraints, top and bottom by vertical constraints.

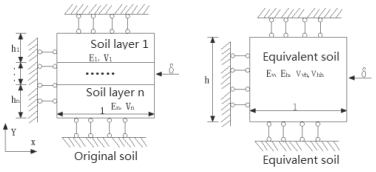

Fig. 4 Equivalent model 2 of Poisson ratio

Using the same method, we can get the following formula:

$$\nu_{vh}(1+\nu_{hh})/(1-\nu_{vh}^2)=(\sum_{i=1}^{n}E_ih_i)(\sum_{i=1}^{n}\frac{h_i}{E_i})\Big/\{h[\sum_{i=1}^{n}\frac{h_i(1-\nu_i)}{\nu_i}]\} \tag{10}$$

The above two equations are simultaneously solved, the poisson ratio in the horizontal direction is:

$$\nu_{vh}=\left\{-1+\left[1+B\left(B-A^{-1}\right)\right]^{-0.5}\right\}\Big/\left(B-A^{-1}\right) \tag{11}$$

And the poisson ratio in the vertical direction:

$$\nu_{hh}=\left\{AB-\left[1+B\left(B-A^{-1}\right)\right]^{-0.5}\right\}\Big/(AB-1) \tag{12}$$

Where, $A=\left(\sum_{i=1}^{n}\lambda_ih_i\right)\Big/R$, $B=R\Big/\left[\sum_{i=1}^{n}(h_i/\lambda_i)\right]$, $R=\left(\sum_{i=1}^{n}E_ih_i\right)\left(\sum_{i=1}^{n}h_i/E_i\right)\Big/h$, $\lambda_i=\nu_i/(1-\nu_i), i=1,2,,,n$

CONSTRUCTION SIMULATION OF TUNNEL EXCAVATION

Model Establishment

Luan Jiayan tunnel of Guangnan highway is 3265 meters long, which is located in north-central Sichuan basin. As for the construction conditions the layers are nearly flat, the attitude of rocks at the tunnel entrance is 280~320° ∠1~3°,the rock is mainly composed of thin-middle siltstone and mudstone interbedding rock mass, and interlayer bonding is poor. With Luan Jiayan tunnel as the research object to establish numerical model, tunnel's buried depth is 150m, and the model is 200m wide, 150m long, and 210m high, every 4m is divided into a unit in longitudinal direction. Vertical displacement constraints are imposed in the lower boundary, the level displacement constraints are applied in the left and right boundary and the axis displacement constraints are applied in the front and behind boundary of the model, as is shown in Figure 5.

Fig. 5 Three dimensional numerical model

According to the geological investigation date for the Luan Jiayan tunnel and the design specification of highway tunnel, there is no groundwater, the property parameters of stratum and primary support are shown in the following Table 1.

Table. 1 Material parameters of numerical model

name	E/MPa	Poisson ratio v	γ/kN·m^{-3}	C/MPa	Φ	ratio %
Mudstone	1500	0.35	19.7	0.14	25	37.5
Siltstone	2800	0.32	22.8	0.4	33	62.5
primary support	23000	0.2	22	--	--	--

By putting the above data into the front of the formula, properties of the equivalent formation can be obtained. The physical property parameters are as following:

E_v=2113MPa; E_h=2312MPa; v_{vh}=0.4095; v_{hh}=0.1764; γ=21.64kN/m3

Excavation Simulation

The benching tunneling construction method is applied in the Luan Jiayan highway tunnel excavation. Compared with the down steps, the up steps are beyond 40 meters. Simulation of the excavation is shown in Figure 6. During the construction, in order to prevent the horizontal rock from blocking and collapsing, the initial support parameters are as follows:

The level of the sprayed concrete: C20

Thickness: 25cm

I-steel model: I18

Interval: 1.0m

The initial support parameters are viewed as an equivalent average shell and then applied to this model. The equivalent physical parameters are shown in Table 1.

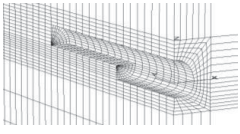

Fig. 6 Simulation of the excavation

Generally, there are 2-blasting cycle every day and there is a drilling and blasting operation cycle almost every 2 meters in the construction, and the initial support must be immediately applied after every time of blasting operation. In the numerical

calculation, it selects 8 meters as an excavation calculation cycle step. Through the construction process simulation, this paper is intended to study the rule of the surrounding rock displacement caused by highway tunnel excavation in the horizontal sandstone and mudstone interbedding rock mass.

Result Analysis

In order to eliminate the influence of the boundary effect, the model longitudinal intermediate position is selected, Y = 100 m, as monitoring section. The situation in which the displacement of the vault, sidewall and inverted arch changed with excavation steps is shown in Figure 7. As can be seen, because the settlement of the vault resulted from the excavation of the upper bench makes up 70% of the total settlements and the uplift quantity in the inverted arch takes up 55% of the total uplift quantities, the excavation of the upper bench would lead to settlement in the vault and uplift in the inverted arch significantly. Likewise, because the convergence magnitude of the sidewall resulted from the excavation of the lower bench makes up 70% of the total convergence displacements, the excavation of the lower bench would lead to the increment of the sidewall convergence. Under the initial support, the finial displacements of edges of tunnel are as follows:

Vault: -19.11mm; Sidewall: -9.45mm; Inverted arch: 6.82mm

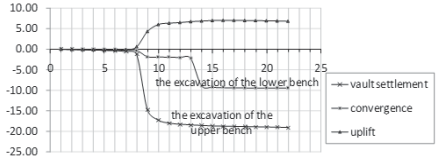

Fig.7 Displacement variation with tunnel excavation

In the model monitoring section, Y=100m, the vertical displacement contours in the final state under the initial support are shown in Figure 8, and the Figure 9 is used to show the horizontal displacement contours.

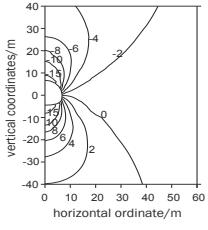

Fig.8 Displacement in vertical direction

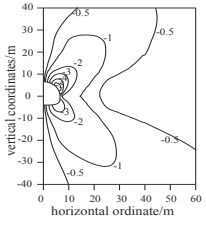

Fig.9 Displacement in horizontal direction

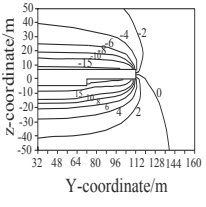

Fig.10 Vertical displacement in the plan x=0

On the basis of the Figure 8 and Figure 9, it can concluded that the biggest vertical displacement in the model longitudinal direction usually occurs in the X=0 plane. When the tunnel is dug through completely, the strata displacement on the longitudinal section reaches the maximum, but the displacement in the longitudinal is uniformly distributed, the uneven displacement is smaller. The strata uneven displacement appears in the excavation stage, especially near the excavation face. When the upper stair excavation surface is located in Y = 112 m, the distribution of vertical displacement in the X=0 plane is shown in Figure 10. As can be seen, the vertical displacement near the upper stair excavation surface changes greatly and the vertical displacement at the distance of three times of diameter to the down stair excavation surface is basically stable.

ANALYSIS OF FIELD TEST RESULTS

It selects cross-section of ZK87+295 mileages which is located in Luan Jiayan tunnel to launch the field testing of displacement around the hole. The buried depth of this cross-section is about 150 meters and the benching tunneling construction method is used to excavate this cross-section. Three measuring points, located in this test cross-section, are used to measure the changes of vault settlement and horizontal convergence in tunnel excavation. Three measuring points are shown in Figure 11.

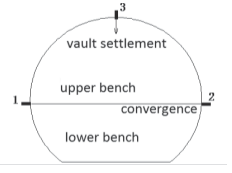

Fig.11 Displacement measuring point around tunnel

After the slag is carried away, the measuring point would be arranged with the steel arch being erected. Initial reading could not be acquired until the shotcreting-bolting support is completed, which does not include the displacement value before shotcreting-bolting support is finished. The measuring point is welded on the steel arch so as to ensure that it completely bond on the frame of initial support. Test frequencies are as follows: early days: once a day and then gradually transit to once two days or once seven days, finally after the inverted arch is closed, the displacement became stable, and test frequency changes to once a month.

The situations in which the settlement of the vault and the horizontal convergence change with excavation steps are shown in Figure 12 and 13. As can be seen, the settlement of the vault and the horizontal convergence mainly are resulted from the excavation of the upper bench. With the advance of the excavated surface, the displacement rate decreases gradually and tends to be stable. The monitoring data shows that the design of the initial support is reasonable. So the initial support can ensure the displacement tend to be stable. After the excavation of the lower bench, the